Published in final edited form as:

Mol Cancer Ther. 2022 January ; 21(1): 38–47. doi:10.1158/1535-7163.MCT-21-0293.

AXL inhibitor TP-0903 reduces metastasis and therapy resistance in pancreatic cancer

Yuqing Zhang[1,2,3,*], **Emily N. Arner**[1,2,3,*], **Ali Rizvi**[1], **Jason E. Toombs**[1,3], **Huocong Huang**[1,3], **Steven L. Warner**[4], **Jason M. Foulks**[4], **Rolf A. Brekken**[1,2,3,5]

[1]Hamon Center for Therapeutic Oncology Research, UT Southwestern, Dallas TX 75390

[2]Cancer Biology Graduate Program, UT Southwestern, Dallas TX 75390

[3]Department of Surgery, UT Southwestern, Dallas TX 75390.

[4]Sumitomo Dainippon Pharma Oncology Inc., Lehi UT 84043

[5]Department of Pharmacology, UT Southwestern, Dallas TX 75390

Abstract

Pancreatic cancer is the 3rd leading cause of cancer-related deaths in the United States with a 5-year survival less than 5%. Resistance to standard therapy and limited response to immune checkpoint blockade due to the immunosuppressive and stroma-rich microenvironment remain major challenges in the treatment of pancreatic cancer. A key cellular program involved in therapy resistance is epithelial plasticity, which is also associated with invasion, metastasis, and evasion of immune surveillance. The receptor tyrosine kinase AXL is a key driver of tumor cell epithelial plasticity. High expression and activity of AXL is associated with poor prognosis, metastasis, and therapy resistance in multiple types of cancer including pancreatic. Here, we show that an AXL inhibitor (TP-0903), has anti-tumor and therapy sensitizing effects in pre-clinical models of pancreatic ductal adenocarcinoma (**PDA**). We demonstrate that TP-0903 as a single agent or in combination with gemcitabine and/or anti-programmed cell death protein 1 (PD1) antibody has anti-metastatic and anti-tumor effects in PDA tumor bearing mice, leading to increased survival. Additionally, gene expression analysis of tumors demonstrated upregulation of pro-inflammatory and immune activation genes in tumors from TP-0903-treated animals compared to the vehicle, indicating pharmacologic inhibition of AXL activation leads to an immunostimulatory microenvironment. This effect was augmented when TP-0903 was combined with gemcitabine and anti-PD1 antibody. These results provide clear rationale for evaluating TP-0903 in the treatment of pancreatic cancer.

Keywords

AXL; metastasis; therapy resistance; pancreatic cancer; epithelial plasticity

Corresponding author: Rolf A. Brekken, PhD, Hamon Center for Therapeutic Oncology Research, UT Southwestern, 6000 Harry Hines Blvd., Dallas, TX 75390-8593, Tel: 214.648.5151; Fax: 214.648.4940, rolf.brekken@utsouthwestern.edu.

*equal contribution

Declarations of interest: RAB received research support from Sumitomo Dainippon Pharma Oncology for these studies; SLW and JMF are employees of Sumitomo Dainippon Pharma Oncology Inc.; The remaining authors do not have potential conflicts of interest.

Introduction

Pancreatic cancer is a deadly cancer in the United States with a 5-year survival of approximately 10%. The high incidence to death ratio is attributed to lack of effective targeted therapies, therapy resistance, and late diagnosis, highlighting the importance of new strategies to overcome these barriers (1). Over 75% of pancreatic cancer patients are diagnosed after the tumor has already advanced locally and metastasized. Cancer metastasis is the leading cause of cancer mortality and has been shown to correlate with epithelial-to-mesenchymal transition (**EMT**), a prominent process that alters gene expression and morphology of tumor cells, resulting in a more invasive and therapy-resistant tumor cell phenotype (2, 3). EMT is a hallmark of metastasis in PDA and is thought to be critical to cancer cell dissemination (4-6).

Many signaling pathways can mediate tumor cell epithelial plasticity, including the receptor tyrosine kinase (**RTK**) AXL (7-9), elevated expression of which correlates with metastasis and resistance to therapy in multiple types of cancers, including pancreatic (7, 10). AXL is a member of the **TAM** (Tyro3, AXL, MerTK) family of RTKs (11) and is activated by its ligand, growth arrest-specific gene 6 (**GAS6**) to promote a variety of cellular processes, including epithelial plasticity, proliferation, and migration (7).

TP-0903 is an orally bioavailable novel small molecule that was originally developed to target AXL (12) by Tolero Pharmaceuticals and is currently, undergoing evaluation in a first-in-human study in patients with advanced solid tumors (CinicalTrials.gov; NCT02729298). TP-0903 is an ATP-competitive inhibitor that possesses an adenine-mimicking heterocyclic moiety and binds to the active conformation of AXL (12). It also targets other kinases including all three members of TAM family (Tyro3, AXL and MerTK) as well as Aurora A, JAK2, ALK, ABL1 and VEGFR2 (13). The structure of TP-0903 has been reported previously (12) and the formation of TP-0903 tartrate salt is shown in Supplementary Figure 1A. Recently additional studies established TP-0903 has potent anti-tumor effects on drug-resistant AML` (14).

Here, we show that TP-0903 has anti-tumor, anti-metastatic and therapy sensitizing effects in orthotopic and genetically engineered mouse models (**GEMMs**) of PDA, leading to prolonged survival. Additionally, gene expression analysis of the tumors demonstrated differential expression of pro-inflammatory and immune activation genes in TP-0903-treated groups compared to the vehicle. This effect was augmented when TP-0903 was used in combination with gemcitabine and/or anti-programmed cell death protein 1 (PD1). These results support the use of TP-0903 in combination with chemo- and/or immunotherapy for treatment of pancreatic cancer.

Materials and Methods

Reagent

TP-0903 tartrate salt (R&D lot number SCR311-17) was produced by PCAS-Nanosyn Inc., in Santa Rosa, CA and provided by Tolero Pharmaceuticals for our studies.

Cell lines

BMF-A3, an isogenic pancreatic cancer cell line, was derived from *KPfC* (*Kras*$^{LSL\text{-}G12D/+}$; *Trp53*$^{lox/lox}$; *Pdx*$^{Cre/+}$) mice in the Brekken Lab. Briefly, the pancreas from a *KPfC* animal with large established disease was minced and digested with a cocktail containing collagenase I (45 μ/ml; Worthington), collagenase II (15 μ/ml; Worthington), collagenase III (45 μ/ml; Worthington), collagenase IV (45 μ/ml; Worthington), elastase (0.075 μ/ml; Worthington), hyaluronidase (30 μ/ml; MilliporeSigma), and DNase type I (25 μ/ml; MilliporeSigma) for 40 minutes at 37°C to obtain a single-cell suspension. The resulting cells were centrifuged at low speed to pellet large debris, resuspended, filterd and plated at low density to isolate tumor cell populations. Cells were confirmed to be tumor cells by immunocytochemistry staining for tumor cell markers and PCR. BMF-A3 was passaged approximately 30 times after isolation and before use in mice. KPC-450, a *KPC* (*Kras*$^{LSL\text{-}G12D/+}$; *Trp53*$^{LSL\text{-}R172H/+}$; *Pdx*$^{Cre/+}$) cell line was a generous gift from Paolo Provenzano (University of Minnesota) and confirmed by immunocytochemistry and PCR. Cells were cultured in DMEM (Invitrogen) containing 5% FBS and maintained at 37°C in a humidified incubator with 5% CO2 and 95% air and confirmed to be mycoplasma free before use.

Animal studies

KPfC (*Kras*$^{LSL\text{-}G12D/+}$; *Trp53*$^{lox/lox}$; *Pdx*$^{Cre/+}$) and *KPC* (*Kras*$^{LSL\text{-}G12D}$; *Trp53*$^{LSL\text{-}R172}$; *Ptf1a*$^{Cre/+}$) mice were enrolled into survival studies and randomized into treatment groups. Therapies were initiated at day 35 for *KPfC* and at day 100 for *KPC* and maintained until animals became moribund at which time animals were sacrificed. Tumor and liver tissues were harvested and evaluated for weight. The survival study consists of 8 treatment groups: vehicle; TP-0903, 25 mg/kg, daily, oral gavage; gemcitabine, 25 mg/kg, ip, 3x/week; anti-PD1 antibody (clone: RMP14-1), 5 mg/kg, ip, twice per week; TP-0903+gemcitabine; TP-0903+anti-PD1; TP-0903+gemcitabine+anti-PD1; gemcitabine+anti-PD1. In the combination group with gemcitabine, TP-0903 was administrated three times per week. In the combination group with anti-PD1 antibody, TP-0903 was given five times per week. In the triple therapy group, TP-0903 was administrated three times per week. In all therapy groups for *KPC* mice, TP-0903 was given three times per week. For orthotopic studies, 0.5×10^6 *KPfC* BMF-A3 cells or 0.25×10^6 KPC-450 cells were implanted orthotopically into WT C57BL/6 mice. Ultrasound was done on a cohort of animals to confirm tumor burden before therapy was initiated. For *KPfC* endpoint study, therapy was initiated at day 10 post tumor cell injection. Treatments consist of 8 groups as mentioned above. All mice were sacrificed on Day 35. For *KPC* survival study, treatments consist of vehicle, TP-0903, gemcitabine+anti-PD1, TP-0903+gemcitabine+anti-PD1. Tissues were fixed in 10% formalin or snap-frozen in liquid nitrogen for further studies. The extent of liver metastasis was determined based on gross metastasis. Macroscopic metastasis was examined based on H&E staining of liver tissues. All animal experiments were done using UT Southwestern Medical Center IACUC approved protocols.

MTS assay

The MTS colorimetric assay (Promega) was performed as per the manufacturer's instructions. Cells were plated on day 0 and TP-0903 was added on day 1 in 4-fold dilutions starting at 40 μM (highest dose). For each assay, 8 different drug concentrations were tested with 8 replicates per concentration. Relative cell number was determined by adding MTS (Promega, Madison, WI, final concentration 333 μg/ml), incubating for 1 to 3 hours at 37°C, and reading absorbance at 490 nm on a plate reader (Spectra Max 190, Molecular Devices, Downingtown, PA). Drug sensitivity curves and IC_{50}s were calculated using in-house software (DIVSA). Response was validated in replicate plates ($n \geq 4$). IC_{50} for BMF-A3 was determined to be 110 nM.

Liquid colony-forming assay

KPfC cells, BMF-A3, were cultured in 6-well culture plates at low density (500 cells/well) in 2 ml media on Day 0. On Day 1, cells were treated with DMSO (control), 100, 250, 500 nM TP-0903, or 5 μM TP-0903. Cells were allowed to settle for 10 days until marked colony formation in control plates. Cells were fixed with 10% formalin and stained with crystal violet. N> 3 for each dose. Colonies were counted and each dose was normalized to the control for that assay and graphed using GraphPad.

Histology and tissue analysis

Formalin-fixed tissues were embedded in paraffin and cut into 5 μm sections. Sections were evaluated by H&E and immunohistochemical analysis using antibodies specific for MPO (R&D, AF3667), F4/80 (Cell Signaling, 70076s), iNOS (invitrogen, PA1-21054), CD8 (Cell Signaling, 98941s), PD1 (Cell Signaling, 84651s), Snail (Cell Signaling, 3879), Ki67 (Abcam, 15580), CD31 (Cell Signaling, 77699), E-Cadherin (Cell Signaling, 3195), vimentin (Cell Signaling, 5741), CK19 (Abcam, 15463) and Zeb1 (Cell Signaling, 3396). Negative controls included omission of primary antibody. Color images were obtained with Hamamatsu Nanozoomer 2.0HT using NDPview2 software. Pictures were analyzed using NIS Elements (Nikon) and Fiji software.

Nanostring analysis

KPfC tumor tissues from orthotopic endpoint experiment were lysed in RLT lysis buffer and purified according to the manufacturer's instructions (QIAGEN). RNA was sent to the Microarray Core Facility in UTSouthwestern and analyzed using a preassembled nCounter PanCancer Immune Profiling Panel (mouse) and the nCounter system (NanoString Technologies) according to the manufacturer's instructions. Samples were then normalized based on the geometric means of the supplied positive controls and the panel of housekeeping genes, as recommended by the manufacturer.

Western blot analysis

BMF-A3 cells were treated with serum-free medium (SFM), 3 nM AF854 (an AXL activating antibody (Cruz, 2019 #196)) or AF854 + 4 uM or 10 uM TP-0903 for 1 hr. KPC-450 cells were treated with SFM, 6 nM AF854, or AF854 + 4 uM TP-0903 for 1 hr. Cells were then lysed using RIPA buffer. Protein concentration was measured using

a Pierce BCA Protein Assay Kit (Thermo Fisher Scientific, 23225), and equal amounts of total protein were separated by SDS-PAGE. Proteins were transferred to nitrocellulose membranes (Bio-Rad), followed by a blocking in 5% BSA in TBST. The membranes were incubated overnight at 4°C with primary antibody, AXL (R&D, AF854), pAKT S473 (Cell Signaling, 4060s), AKT (Cell Signaling, 9272s), Slug (Cell Signaling, 9585)and GAPDH (Cell Signaling, 4118) followed by corresponding horseradish peroxidase–conjugated secondary antibody (Jackson ImmunoResearch). In BMF-A3 cells, precipitation was performed and pull-down samples and respective whole cell lysates were immunoblotted with anti-AXL (R&D, AF854) and anti-phosphotyrosine (Upstate, 05-321) antibodies. Specific bands were detected by using WesternSure PREMIUM chemiluminescent substrate (Li-Cor) on a Li-Cor imaging system (Odyssey-Fc). Three biological replicates were performed.

Statistics

Data are reported as mean ± SEM. Statistical analysis was performed with a 2-tailed t test or ANOVA using GraphPad Prism software. For all analyses, $P < 0.05$ was considered statistically significant.

Data Availability Statement

The data generated in this study are within the article and its supplementary data files. Data from Nanostring analysis are publicly available in Gene Expression Omnibus (GEO) at GSE185110.

Results

AXL inhibitor TP-0903 sensitizes *KPfC* GEMM mice to chemotherapy and immune checkpoint blockade.

We evaluated the antitumor efficacy of TP-0903 in ***KPfC*** (*Kras*$^{LSL\text{-}G12D}$; *Trp53*$^{fl/fl}$; *Pdx*$^{Cre/+}$) mice, a GEMM of PDA. TP-0903 dosing was initiated when established tumors were visible by ultrasound (~Day 35). Animals were monitored daily until they were moribund. The median survival for *KPfC* mice treated with vehicle was 72 days. TP-0903 as a single agent extended median survival to 78 days and significantly reduced tumor weight at the time of sacrifice (Figure 1A). Given that chemotherapy is currently the standard of care for PDA (15), we evaluated the benefit of combining TP-0903 and gemcitabine in *KPfC* mice. Although gemcitabine improved the median survival of *KPfC* mice (89.5 days, $p<0.01$ vs control), combination with TP-0903 was more effective with a median survival of 92.5 days ($p<0.01$) and reduced tumor size at the time of sacrifice more effectively than gemcitabine alone (Figure 1B).

PDA is typically characterized as an immunologically “cold” tumor. Consistent with this, PDA has remained largely refractory to immune checkpoint blockade (16). The immunosuppressive and stroma-rich microenvironment is a major limitation for the efficacy of cancer immunotherapy in PDA patients (17, 18). We evaluated the effect of anti-PD1 in *KPfC* mice and found it did not improve survival or reduce tumor weight compared to vehicle (Figure 1C). However, anti-PD1 therapy in combination with TP-0903 improved the

median survival to 85 days, a significant improvement compared to anti-PD1 therapy alone ($p = 0.0041$ vs anti-PD1) (Figure 1C and Table 1). Given that the dual combination therapy regimens were tolerable we investigated the tolerability and efficacy of combining TP-0903, gemcitabine and anti-PD1 in *KPfC* mice. The triple therapy improved median survival to 95.5 days ($p = 0.0002$ vs vehicle; $p = 0.08$ vs gemcitabine) and was the most effective therapy regimen out of the 8 tested compared to vehicle (Figure 1D and Table 1). At the time of sacrifice, the tumor weight in triple therapy group was significantly decreased ($p < 0.01$) compared to tumors from gemcitabine group and gemcitabine + anti-PD1 group (Figure 1D).

Taken together, the survival study in the *KPfC* GEMM demonstrates that TP-0903 sensitizes PDA to chemotherapy and immune checkpoint blockade, leading to a significant anti-tumor and pro-survival effect in a GEMM of PDA.

TP-0903 is effective as a single agent or in combination with chemo- and immunotherapy and promotes an immune stimulatory microenvironment in a syngenic model of PDA.

To investigate the effect of TP-0903 on control of tumor growth and metastasis we performed an end-point study using an orthotopic syngenic model. BMF-A3, an isogenic *KPfC* PDA cell line with moderate to high metastatic capacity, was implanted orthotopically in C57BL/6 mice. Ultrasound was performed on a cohort of animals to confirm tumor burden (tumor size: 2-5 mm in one dimension) before therapy was initiated at day 10 post tumor cell injection. Eight therapy cohorts (n=7-9/group) as displayed in Figure 1 were enrolled. All mice were sacrificed on day 35 after tumor cell injection. TP-0903 was demonstrated to inhibit AXL phosphorylation in a dose dependent manner in BMF-A3 cells (Supplementary Figure 1B).

Consistent with the *KPfC* survival study, TP-0903 as a single agent suppressed tumor growth significantly (Figure 2A). TP-0903 in combination with gemcitabine and/or anti-PD1 antibody did not significantly improve tumor growth inhibition compared to TP-0903 alone, although tumor weights from the triple combination group exhibited tighter distribution (Figure 2A). At the time of sacrifice, the extent of liver metastasis was determined based on gross metastasis. Five out of 8 evaluable mice in the vehicle group had at least 1 macroscopic metastasis. Gemcitabine or anti-PD1 alone did not reduce the number of mice with gross metastasis. In contrast, TP-0903 as single agent decreased the gross metastasis incidence from 62.5% to 14.3% (Figure 2B and Table 2). Combination therapy TP-0903 + gemcitabine or TP-0903 + anti-PD1 antibody further reduced gross metastasis incidence and the triple therapy eliminated macrometastasis in all animals (n=9) (Figure 2B and Table 2). Figure 2C displays example H&E staining of serial liver tissues from vehicle and TP-0903 treated groups (n=5/group). In all five animals from vehicle treated group, we observed histological micrometastasis while this number was reduced to 2/5 in TP-0903 alone treatment group (Figure 2C).

Given the potent anti-tumor activity of TP-0903 and survival benefits of TP-0903 in combination with anti-PD1 and gemcitabine, we performed gene expression/program and pathway analysis (NanoString Technologies) using frozen tumor tissues collected from the orthotopic *KPfC* (BMF-A3) implant model. TP-0903 treatment showed a slight

upregulation in inflammatory and immune active pathways compared to the vehicle, while the combination groups with gemcitabine or anti-PD1 revealed more distinct activation in those pathways compared to single agent therapy (Figure 2D).

To confirm the results of pathway analysis, we further evaluated tumor tissues from the orthotopic *KPfC* implant model. Consistently, we found a decrease of tumor-associated neutrophil and macrophage infiltration (characterized by MPO and F4/80 expression) in tumors with combination therapies or TP-0903 alone (Figure 2E and F). Furthermore, the infiltrated macrophages exhibited enhanced immunostimulatory phenotype as iNOS expression was elevated in combination therapies as well. The combo treatment of TP-0903 and gemcitabine showed the most significant effects in regulating iNOS expression compared to TP-0903 single agent and gemcitabine alone (Figure 2E and F). Meanwhile, the $CD8^+$ T cell infiltration was increased slightly by TP-0903 alone and further elevated by gemcitabine or combination therapies although there were few T cells in the orthotopic *KPfC* model (Supplementary Figure 1C). Interestingly, PD1 expression on T cells was upregulated by TP-0903 treatment as well as TP-0903 in combined with gemcitabine and accordingly, with anti-PD1 antibody on board, PD1 expression went down to a relatively low level again (Supplementary Figure 1C and D).

These data confirmed the efficacy of TP-0903 in control of tumor growth in an aggressive model of PDA. These observations also suggest TP-0903 is potent in limiting metastasis as a single agent or in combination with chemo- or immunotherapy in a syngenic model of PDA. Importantly, TP-0903 alone or in combination with gemcitabine and anti-PD1 facilitates immune activation in an immunologically “cold” syngenic model of PDA.

TP-0903 induces a more differentiated tumor cell phenotype in *KPfC* GEMM model.

To demonstrate the effect of TP-0903 on tumor cell viability, we performed *in vitro* MTS viability and colony formation assays. TP-0903 inhibited BMF-A3 cell viability with an IC_{50} of 0.11 μM (Figure 3A) and reduced colony formation in a dose-dependent manner (Figure 3B).

Immunohistochemistry analysis of tumors from the *KPfC* survival study was performed to evaluate tumor cell phenotype *in vivo*. Consistent with the effect of TP-0903 on tumor cells *in vitro*, Ki67 expression was suppressed with TP-0903 treatment as single agent. TP-0903 combination with gemcitabine or triple therapy with gemcitabine and anti-PD1 further enhanced this effect with the triple therapy resulting in the most significant changes ($p < 0.01$ vs control) (Figure 3C and D). Since TP-0903 has significant activity against VEGFR2 (13), we also evaluated microvessel density marked by CD31 expression in the *KPfC* tumors. Reduced microvessel density was observed with TP-0903 treatment and the combination strategies led to more robust suppression (Figure 3C and D). Furthermore, TP-0903 treatment resulted in a shift towards a more differentiated tumor cell phenotype evidenced by elevated expression of E-Cadherin and a decreased number of vimentin-positive cells. Although the increase in E-Cadherin expression was similar among all TP-0903 combination groups, vimentin expression was further decreased in the triple therapy group compared to gemcitabine alone (Figure 3C and D). Snail, which is an EMT- transcription factor (**EMT-TF**)(19), was also decreased when mice were treated by

TP-0903 alone or in combination with gemcitabine *in vivo* (Supplementary Figure 2A). Taken together, these results suggest TP-0903 regulates critical pathways supporting tumor progression in the tumor microenvironment *in vivo*.

TP-0903 in combination with chemo- and immunotherapy leads to extended survival in a refractory syngenic model of PDA.

To extend our observations, we performed a similar survival study in *KPC* (*Kras*$^{LSL\text{-}G12D}$; *Trp53*$^{LSL\text{-}R172}$; *Ptf1a*$^{Cre/+}$) mice, a GEMM which has a longer median survival of ~150 days, develops metastasis in 30-40% of animals and resembles the progression of human PDA (20). The *KPC* model is heterogeneous in tumor onset and progression. Treatment of TP-0903 as single agent slightly extended the median survival of animals although it did not reach significance (Supplementary Figure 3A). Addition of TP-0903 to gemcitabine or anti-PD1 did not improve efficacy. The triple combination therapy also did not improve survival compared to single agent gemcitabine therapy. We did observe that gemcitabine alone or in combination with TP-0903 reduced metastatic incidence (Supplementary Figure 3B-D). Tissue analysis of *KPC* tumors from different treatment groups did not show significant changes in Ki67, CD31, E-Cadherin or vimentin expression for any group (Supplementary Figure 4A and B).

To investigate efficacy of TP-0903 in a *KPC*-based model we performed a survival experiment in C57BL/6 mice bearing orthotopic *KPC* tumors from a cell line derived from *KPC* mice. Treatment groups consisted of vehicle, TP-0903, gemcitabine+anti-PD1, TP-0903+gemcitabine+anti-PD1 and started when tumors were established (day 10 post tumor cell injection). Mice were sacrificed when they were moribund. TP-0903 and gemcitabine + anti-PD1 therapy had insignificant effects on median survival (the median survival for vehicle was 29 days, TP-0903 was 33 days, and Gem + anti-PD1 was 36 days); however, median survival in the triple combination therapy group was longer (38.5 days) with 30% of the mice showing extended survival (Figure 4A). In addition, consistent with the *KPfC* model, TP-0903 in combination with chemo- and immunotherapy significantly reduced primary tumor size (Figure 4B). In contrast to the *KPfC* implant model, therapy (of any kind or combination) did not reduce metastatic burden or incidence (Figure 4B). Histological analysis revealed TP-0903 therapy alone or in the triple therapy group induced a more differentiated tumor cell phenotype with elevated E-Cadherin expression and decreased vimentin expression compared to the control (Figure 4C). When we evaluated CK19, and Zeb1, a mesenchymal cell marker, we found significantly elevated CK19 and a trend towards decreased Zeb1 expression in the triple therapy group compared to the control, further supporting the findings that TP-0903 induces a more differentiated state (Supplementary Figure 4C and D). Since we observed a clear difference of survival in the triple therapy group, we evaluated the histology of tumors from long (responders) and short (non-responders) survivors. Interestingly, tumors from these two subtypes within the triple therapy group exhibited contrasting expression of Ki67, E-Cadherin and vimentin. Tumors from responding mice showed reduced Ki67^{+} cells, broader E-Cadherin expression and decreased vimentin expression in contrast to the non-responders (Figure 4D). To further study the downstream signaling of TP-0903 inhibition, we stimulated AXL in KPC-450 cells with an AXL activating antibody (AF854) and inhibited AXL with TP-0903 treatment.

When AXL was stimulated, we found that phosphorylation of AKT was elevated, as expected (21). However, when AXL was inhibited with TP-0903, pAKT was reduced (Figure 4E). In addition, the EMT-TF slug was upregulated when AXL was stimulated but this was blocked by TP-0903 treatment (Figure 4E) supporting the efficacy of AXL targeting using TP-0903. Consistent with the immune activation effects of combination therapies in *KPfC* implant model, TP-0903 as single agent limited tumor-associated macrophages infiltration and the effects were more significant in the triple therapy group (Figure 4F). In addition, iNOS expression as the marker of immune stimulatory phenotype of macrophages was increased in the triple therapy group (Figure 4F). These data highlight the potential efficacy of combination therapy in refractory PDA.

Discussion

Our data show that TP-0903, a small molecule inhibitor of AXL has anti-tumor, anti-metastatic and therapy sensitizing effects in pre-clinical models of pancreatic cancer.

Analysis of tumors from each model and, in particular, in responding tumors demonstrated TP-0903 treatment results in a shift towards a more differentiated tumor phenotype. Consistent with a reduction in epithelial plasticity we found that TP-0903 alone or in combination with chemo and immunotherapy drove an upregulation in inflammatory and immune pathways. Taken together, these results suggest TP-0903 is effective at impinging critical pathways that support tumor progression *in vivo*. While we hypothesize this modulation occurs through the inhibition of AXL, TP-0903 does inhibit other kinases (13) and therefore inhibition of non-AXL targets might contribute to the efficacy of TP-0903. Further studies are needed to evaluate the downstream pathways in PDA effected by TP-0903.

While we did see consistent results with *KPfC* GEMM and the *KPfC* implant model, similar experiments in the *KPC* model were not as consistent. Although the orthotopic *KPC* model did show survival and anti-tumor benefit with TP-0903 on board, the *KPC* GEMM was resistant to therapy. We hypothesize that the therapy resistance of the *KPC* GEMM is due to the heterogeneous tumor development and progression in this model (20), which is supported by the at least partial response that was seen in the *KPC* implant studies. Interestingly, in the KPC orthotopic implant study although TP-0903 alone did not extend the median survival, roughly 30% of the mice in the triple therapy group demonstrated a noticeable survival benefit. Additionally, tumors from long survivors expressed markers consistent with a less malignant tumor status, suggesting different responses to therapy. Our data in the *KPC* orthotopic model confirmed the efficacy of TP-0903 especially in combination with chemo-and immunotherapy as shown in *KPfC* GEMM and orthotopic models and provide a rationale that this combination strategy may be beneficial in therapy resistant tumors.

Another potential explanation for the differential effect between the *KPfC* and *KPC* GEMMs is the TP53 status of these models. PDA tumors in *KPfC* mice are homozygous null for TP53 while tumors in *KPC* mice have a point mutation at R172. As TP53 is a tumor suppressor that induces growth arrest or apoptosis (22), tumors lacking TP53 often display

a higher proliferative index (23). Further investigation is needed to understand if a higher proliferative rate results in better response to TP-0903. Additionally, given the increase in efficacy of TP-0903 in *KPfC* mice, clinical studies are needed to determine if pancreas cancer patients with a full deletion of TP53, which occurs in about 8% of pancreas patients (24), would be better candidates to receive TP-0903.

In summary, we demonstrated that AXL inhibition via treatment with the orally bioavailable compound TP-0903 sensitizes pancreatic tumors to chemo- and immune-therapy in multiple mouse models of PDA. These data suggest that in pancreas cancer patients the effectiveness of therapy will depend on a spectrum of features including oncogenotype and the tumor microenvironment.

Supplementary Material

Refer to Web version on PubMed Central for supplementary material.

Acknowledgements

This work was supported by a sponsored research agreement from Sumitomo Dainippon Pharma Oncology, NIH U54 CA210181 (Project 2), the Effie Marie Cain Fellowship to R. Brekken and NIH F99 CA253718 to E. Arner. We thank Dr. Paolo Provenzano for provision of the KPC cell line. We acknowledge helpful input from Dr. Jill Westcott and members of the Brekken lab.

References

1. Hezel AF, Kimmelman AC, Stanger BZ, Bardeesy N, and Depinho RA. Genetics and biology of pancreatic ductal adenocarcinoma. Genes Dev. 2006;20(10):1218–49. [PubMed: 16702400]
2. Wang Z, Li Y, Ahmad A, Banerjee S, Azmi AS, Kong D, et al. Pancreatic cancer: understanding and overcoming chemoresistance. Nat Rev Gastroenterol Hepatol. 2011;8(1):27–33. [PubMed: 21102532]
3. Tran DD, Corsa CA, Biswas H, Aft RL, and Longmore GD. Temporal and spatial cooperation of Snail1 and Twist1 during epithelial-mesenchymal transition predicts for human breast cancer recurrence. Mol Cancer Res. 2011;9(12):1644–57. [PubMed: 22006115]
4. Gaianigo N, Melisi D, and Carbone C. EMT and Treatment Resistance in Pancreatic Cancer. Cancers (Basel). 2017;9(9).
5. Puls TJ, Tan X, Whittington CF, and Voytik-Harbin SL. 3D collagen fibrillar microstructure guides pancreatic cancer cell phenotype and serves as a critical design parameter for phenotypic models of EMT. PLoS One. 2017;12(11):e0188870. [PubMed: 29190794]
6. Wang S, Huang S, and Sun YL. Epithelial-Mesenchymal Transition in Pancreatic Cancer: A Review. Biomed Res Int. 2017;2017:2646148. [PubMed: 29379795]
7. Kirane A, Ludwig KF, Sorrelle N, Haaland G, Sandal T, Ranaweera R, et al. Warfarin Blocks Gas6-Mediated Axl Activation Required for Pancreatic Cancer Epithelial Plasticity and Metastasis. Cancer Res. 2015;75(18):3699–705. [PubMed: 26206560]
8. Koorstra JB, Karikari CA, Feldmann G, Bisht S, Rojas PL, Offerhaus GJ, et al. The Axl receptor tyrosine kinase confers an adverse prognostic influence in pancreatic cancer and represents a new therapeutic target. Cancer Biol Ther. 2009;8(7):618–26. [PubMed: 19252414]
9. Gjerdrum C, Tiron C, Hoiby T, Stefansson I, Haugen H, Sandal T, et al. Axl is an essential epithelial-to-mesenchymal transition-induced regulator of breast cancer metastasis and patient survival. Proc Natl Acad Sci U S A. 2010;107(3):1124–9. [PubMed: 20080645]
10. Ludwig KF, Du W, Sorrelle NB, Wnuk-Lipinska K, Topalovski M, Toombs JE, et al. Small-Molecule Inhibition of Axl Targets Tumor Immune Suppression and Enhances Chemotherapy in Pancreatic Cancer. Cancer Res. 2018;78(1):246–55. [PubMed: 29180468]

11. Du W, and Brekken RA. Does Axl have potential as a therapeutic target in pancreatic cancer? Expert Opin Ther Targets. 2018;22(11):955–66. [PubMed: 30244621]
12. Shen Y, Chen X, He J, Liao D, and Zu X. Axl inhibitors as novel cancer therapeutic agents. Life Sci. 2018;198:99–111. [PubMed: 29496493]
13. Mollard A, Warner SL, Call LT, Wade ML, Bearss JJ, Verma A, et al. Design, Synthesis and Biological Evaluation of a Series of Novel Axl Kinase Inhibitors. ACS Med Chem Lett. 2011;2(12):907–12. [PubMed: 22247788]
14. Jeon JY, Buelow DR, Garrison DA, Niu M, Eisenmann ED, Huang KM, et al. TP-0903 is active in models of drug-resistant acute myeloid leukemia. JCI Insight. 2020;5(23).
15. Wolfgang CL, Herman JM, Laheru DA, Klein AP, Erdek MA, Fishman EK, et al. Recent progress in pancreatic cancer. CA Cancer J Clin. 2013;63(5):318–48. [PubMed: 23856911]
16. Feng M, Xiong G, Cao Z, Yang G, Zheng S, Song X, et al. PD-1/PD-L1 and immunotherapy for pancreatic cancer. Cancer Lett. 2017;407:57–65. [PubMed: 28826722]
17. Feig C, Gopinathan A, Neesse A, Chan DS, Cook N, and Tuveson DA. The pancreas cancer microenvironment. Clin Cancer Res. 2012;18(16):4266–76. [PubMed: 22896693]
18. Foley K, Kim V, Jaffee E, and Zheng L. Current progress in immunotherapy for pancreatic cancer. Cancer Lett. 2016;381(1):244–51. [PubMed: 26723878]
19. Kokudo T, Suzuki Y, Yoshimatsu Y, Yamazaki T, Watabe T, and Miyazono K. Snail is required for TGFbeta-induced endothelial-mesenchymal transition of embryonic stem cell-derived endothelial cells. J Cell Sci. 2008;121(Pt 20):3317–24. [PubMed: 18796538]
20. Westphalen CB, and Olive KP. Genetically engineered mouse models of pancreatic cancer. Cancer J. 2012;18(6):502–10. [PubMed: 23187836]
21. Cruz VH, Arner EN, Du W, Bremauntz AE, and Brekken RA. Axl-mediated activation of TBK1 drives epithelial plasticity in pancreatic cancer. JCI Insight. 2019;5.
22. Levy N, Yonish-Rouach E, Oren M, and Kimchi A. Complementation by wild-type p53 of interleukin-6 effects on M1 cells: induction of cell cycle exit and cooperativity with c-myc suppression. Mol Cell Biol. 1993;13(12):7942–52. [PubMed: 8247009]
23. Kim MP, and Lozano G. Mutant p53 partners in crime. Cell Death Differ. 2018;25(1):161–8. [PubMed: 29099488]
24. Cicenas J, Kvederaviciute K, Meskinyte I, Meskinyte-Kausiliene E, Skeberdyte A, and Cicenas J. KRAS, TP53, CDKN2A, SMAD4, BRCA1, and BRCA2 Mutations in Pancreatic Cancer. Cancers (Basel). 2017;9(5).

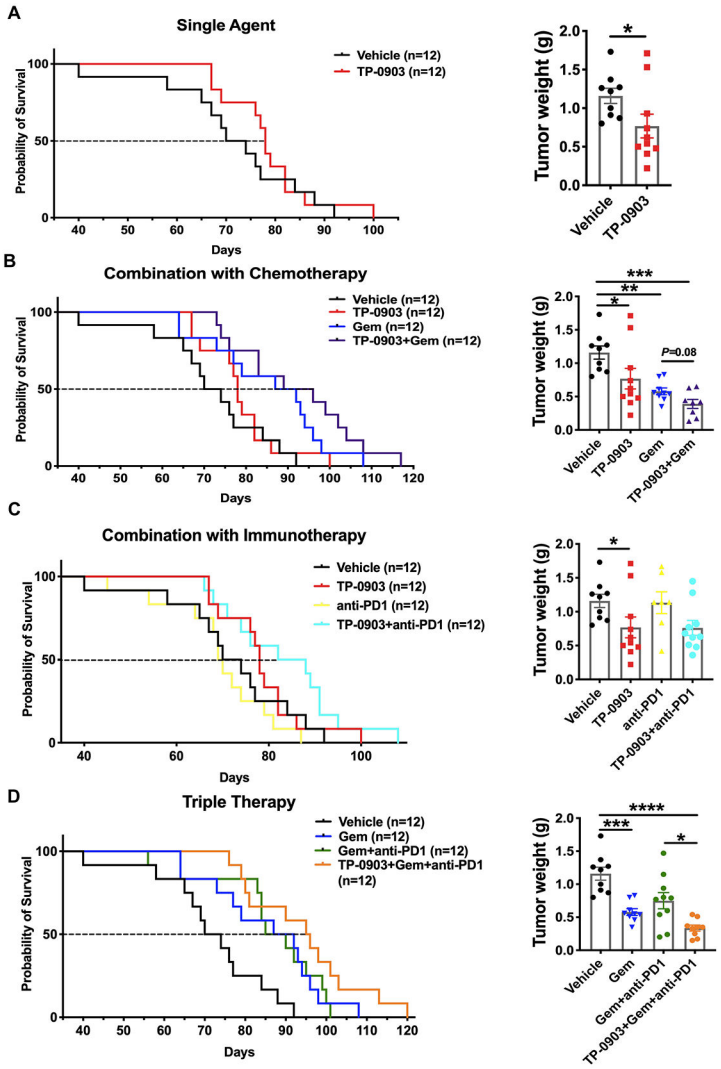

Figure 1. AXL inhibitor TP-0903 sensitizes *KPfC* GEMM mice to chemotherapy and immune checkpoint blockade.

KPfC (*Kras*$^{LSL\text{-}G12D/+}$; *Trp53*$^{lox/lox}$; *Pdx*$^{Cre/+}$) mice were enrolled and randomized into 8 treatment cohorts. Therapies were initiated at day 35 and maintained until animals became moribund at which time animals were sacrificed. Survival curves and final tumor weights are shown. **A)** TP-0903, 25 mg/kg was administered by oral gavage daily. **B)** Gemcitabine: 25 mg/kg, ip, 3x/week. In the combination group with gemcitabine, TP-0903 was administered three times per week, 25 mg/kg. **C)** Anti-PD1 antibody (clone: RMP14-1): 5 mg/kg, ip, twice per week. In the combination group with anti-PD1 antibody, TP-0903 was given five times per week, 25 mg/kg. **D)** In the therapy group of TP-0903+Gem+anti-PD1, TP-0903 was administered three times per week, 25 mg/kg. Tumor weight data are displayed as mean with SEM. *, P<0.05; **, P < 0.01; ***P < 0.005; ****, P < 0.0001; by ANOVA with Tukey's MCT.

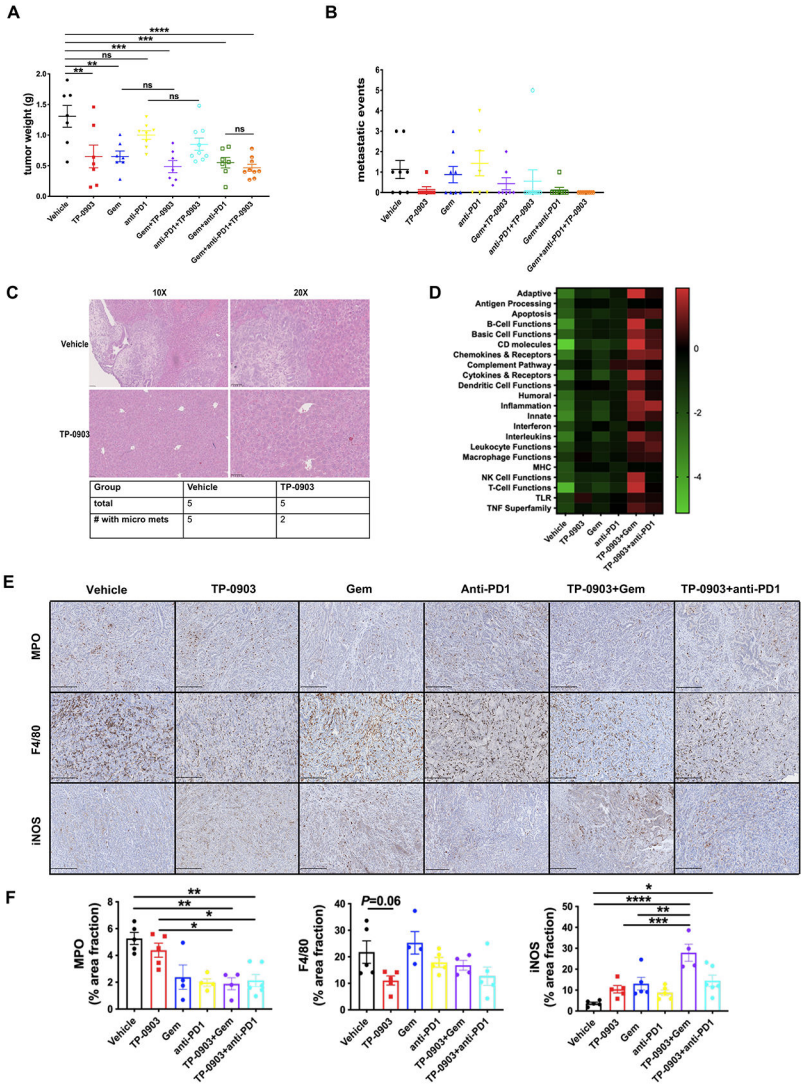

Figure 2. TP-0903 is effective as a single agent or in combination with chemo- and immunotherapy and promotes an immune stimulatory microenvironment in a syngenic model of PDA.

250K *KPfC* cells (BMF-A3) were implanted orthotopically into WT C57BL/6 mice. Therapy was initiated at day 10 post tumor cell injection. Treatments consisted of 8 groups: vehicle; TP-0903, 25 mg/kg, daily, oral gavage; gemcitabine, 25 mg/kg, ip, 3x/week; anti-PD1 antibody (clone: RMP14-1), 5 mg/kg, ip, twice per week; TP-0903+gemcitabine; TP-0903+anti-PD1; TP-0903+gemcitabine+anti-PD1; gemcitabine+anti-PD1. All mice were sacrificed on Day 35 and tumor burden was evaluated. **A, B)** Tumor burden is shown as primary tumor weight (A) and metastatic events (B) determined by gross observation. Data are displayed as mean with SEM. **, $P < 0.01$; ***$P < 0.005$; ****$P < 0.0001$; by ANOVA with Tukey's MCT. **C)** H&E analysis of liver tissue vehicle and TP-0903 treated groups (n=5/group). Representative images were shown. Scale bar, 100 μm or 50 μm. **D)** RNA isolated from *KPfC* orthotopic tumors was analyzed using Mouse PanCancer Immune Profiling Panel (NanoString Technologies). Upregulated (Red) and downregulated (Green) gene programs/functions are shown. **E)** Tumor tissues from *KPfC* orthotopic model treated

with vehicle, TP-0903, gemcitabine, anti-PD1, TP-0903+gemcitabine, TP-0903+anti-PD1 were evaluated by IHC for MPO, F4/80 and iNOS. Representative images are shown. Scale bar, 250 μm. Images were obtained with Hamamatsu Nanozoomer 2.0HT using NDPview2 software. **F)** Images were analyzed using ImageJ software. Quantification of % area fraction is shown. *, $P<0.05$; **, $P < 0.01$; *** $P < 0.005$; **** $P < 0.0001$; by ANOVA with Tukey's MCT.

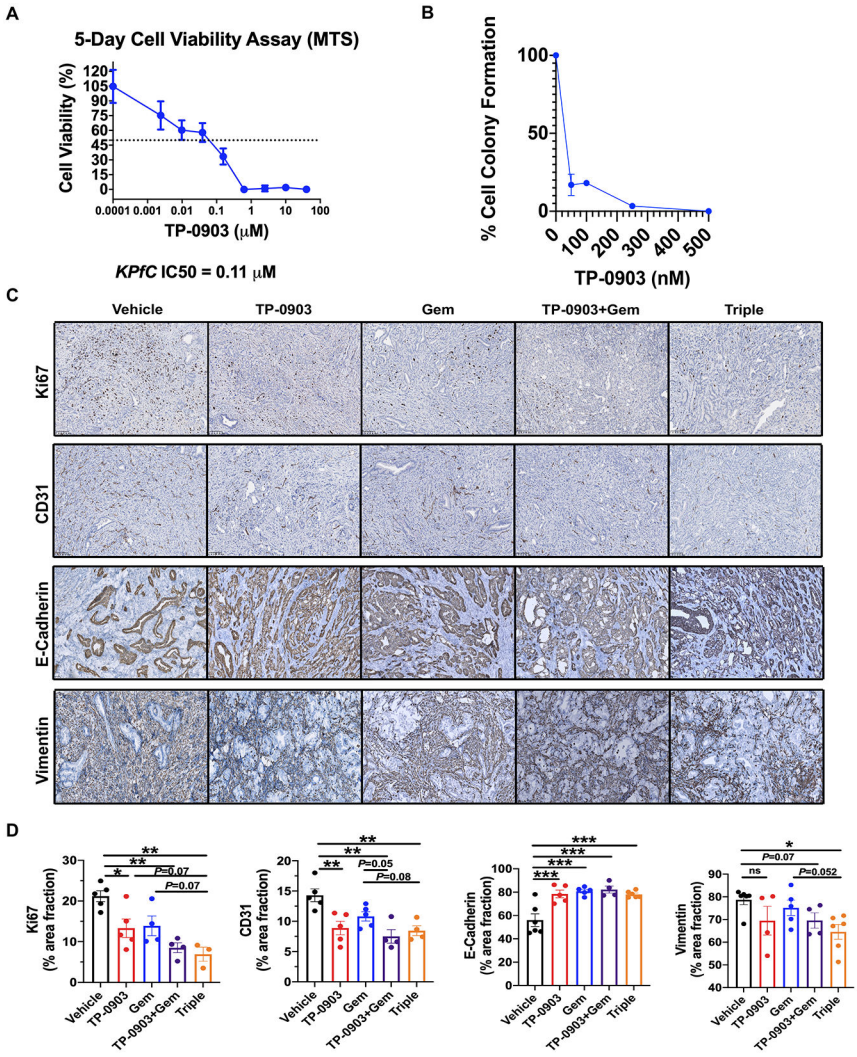

Figure 3. TP-0903 induces a differentiated tumor cell phenotype in *KPfC* GEMM model.

A) IC_{50} for TP-0903 in *KPfC* cells (BMF-A3) was determined by MTS assay. Response was validated in replicate plates ($n \geq 4$). IC_{50} for BMF-A3 was determined to be 110 nM. **B)** BMF-A3 were plated at low density for colony forming assay. Cells were treated with DMSO or TP-0903 at 100, 250, 500 nM or 5 μM. After 10 days, cells were fixed with 10% formalin and stained with crystal violet. N> 3 for each dose. Colonies were counted and each dose was normalized to the control. **C)** Tumor tissues from *KPfC* mice treated with vehicle, TP-0903, gemcitabine, TP-0903+gemcitabine, TP-0903+gemcitabine+anti-PD1 were evaluated by IHC for Ki67, CD31, E-Cadherin and vimentin. Scale bar, 100 μm. Images were analyzed using ImageJ software. Quantification of % area fraction is shown in **D)**. *, $P<0.05$; **, $P < 0.01$; ***$P < 0.005$; by ANOVA with Tukey's MCT.

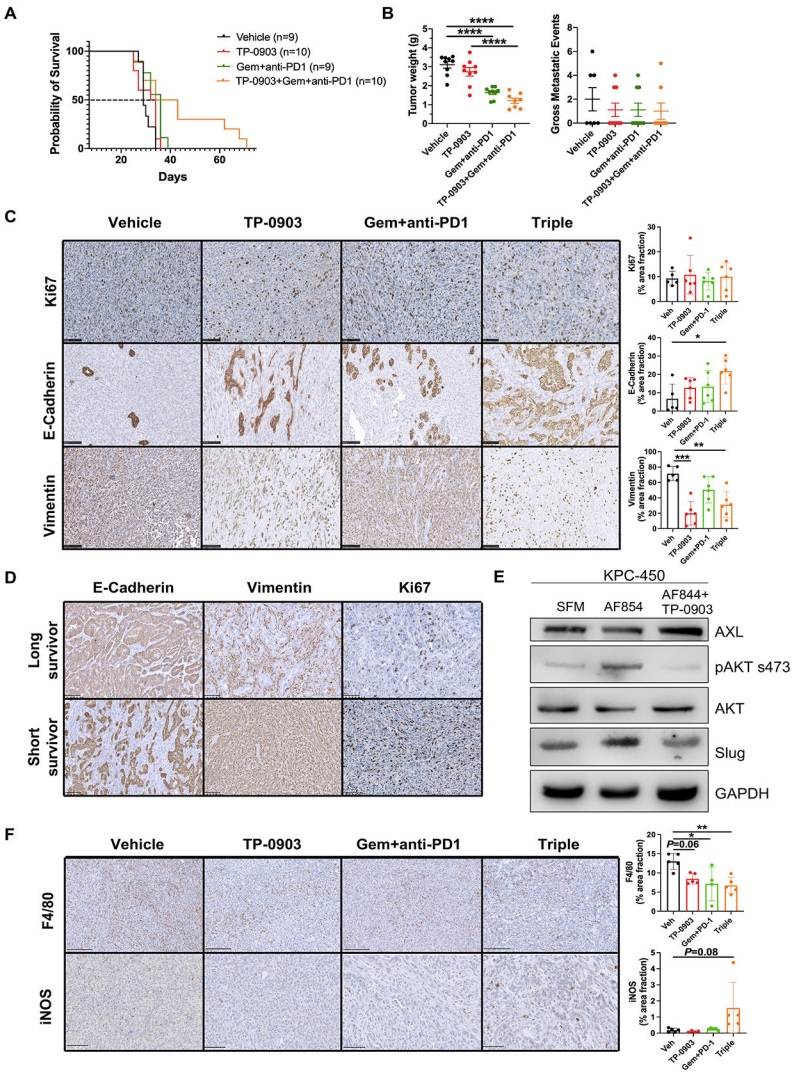

Figure 4. TP-0903 in combination with chemo- and immunotherapy leads to extended survival benefit in a refractory syngenic model of PDA.

250K *KPC* cells were implanted orthotopically into WT C57BL/6 mice. Therapy was initiated at day 7 post tumor cell injection. Treatments consisted of 4 groups: vehicle; TP-0903, 25 mg/kg, oral gavage, 3x/week; gemcitabine (25 mg/kg, ip, 3x/week) + anti-PD1 antibody (clone: RMP14-1, 5 mg/kg, ip, twice per week); TP-0903+gemcitabine+anti-PD1. Mice were sacrificed when they were moribund. **A)** Survival curve is shown. **B)** Tumor and liver tissues were harvested upon sacrifice and evaluated for weight and gross metastasis. Data are displayed as mean ± SEM. ****$P < 0.0001$; by ANOVA with Tukey's MCT. **C)** Tumor tissue from each group were evaluated for Ki67, E-Cadherin and vimentin by IHC. Scale bar, 100 μm. Images were analyzed using ImageJ software. Quantification of % area fraction is shown. *, $P<0.05$; **, $P < 0.01$; ***$P < 0.005$; by ANOVA with Tukey's MCT. **D)** Tumor tissue from long and short survivors in the triple combination therapy group were analyzed for Ki67, E-Cadherin and vimentin. Representative images are shown. Scale bar, 100 μm. Images were obtained with Hamamatsu Nanozoomer 2.0HT using NDPview2 software. **E)** KPC-450 cells were treated with either serum-free medium (SFM), 6 nM

AF854 (activating Axl antibody), or AF854 + 4 μM TP-0903 for 1 hr. Downstream signaling and EMT targets were subsequently probed by western blot. Three biological replicates were done. **F)** Tumor tissue from each group were evaluated for F4/80 and iNOS by IHC. Scale bar, 250 μm. Images were analyzed using ImageJ software. Quantification of % area fraction is shown to the right. *, $P<0.05$; **, $P < 0.01$; by ANOVA with Tukey's MCT.

Table 1.

Median survival summary of all therapy groups in *KPfC* GEMM mice.

Data Summary	Vehicle	TP-0903	Gem	anti-PD1	TP-0903 +Gem	TP-0903 +anti-PD1	Gem+anti-PD1	TP-0903 +Gem+anti-PD1
Median survival	72	78	89.5	69.5	92.5	85	87.5	95.5
P value vs. Vehicle	NA	0.19	0.0095	0.267	0.0016	0.06 (*P*=0.0041 vs. anti-PD1)	0.0082	0.0002 (*P*=0.08 vs. Gem)

Table 2.

Gross metastatic incidence of all therapy groups in *KPfC* syngenic model of PDA.

Gross metastatic incidence								
Group	**Vehicle**	**TP-0903**	**Gem**	**anti-PD1**	**TP-0903 +Gem**	**TP-0903 +anti-PD1**	**Gem+anti-PD1**	**TP-0903 +Gem+anti-PD1**
Total	8	7	8	7	7	9	8	9
# with mets	5	1	4	4	2	1	1	0
metastatic incidence	62.5%	14.3%	50.0%	57.1%	28.6%	11.1%	12.5%	0.0%